5918 *J. Phys. Chem. A* **2002,** *106,* 5918−5923

Absolute Configuration and Conformational Stability of (*S*)-(+)-3-(2-Methylbutyl)thiophene and (+)-3,4-Di[(*S*)-2-methylbutyl)]thiophene and Their Polymers

Feng Wang,† Prasad L. Polavarapu,*,† France Lebon,‡ Giovanna Longhi,‡ Sergio Abbate,‡ and Marinella Catellani§

Department of Chemistry, Vanderbilt University, Nashville, Tennessee 37235, Dip. di Scienze Biomediche e Biotecnologie, Università di Brescia, Via Valsabbina 19, 25123 Brescia (Italy) and Istituto Nazionale di Fisica della Materia (INFM), UdR−Brescia (Italy), and Istituto di Chimica delle Macromolecole, CNR, Via Bassini 15, 20133 Milano (Italy)

Received: December 20, 2001; In Final Form: April 12, 2002

Enantiopure (+)-3-(2-methylbutyl)thiophene **I** and (+)-3,4-di(2-methylbutyl)thiophene **II** and their polymers were prepared using literature procedures and investigated using vibrational circular dichroism (VCD). Experimental absorption and VCD spectra of (+)-3-(2-methylbutyl)thiophene, (+)-3,4-di(2-methylbutyl)-thiophene, and their polymers in $CDCl_3$ solution were recorded in the 2000−900 cm^{-1} region, and the experimental absorption and VCD spectra of (+)-3-(2-methylbutyl)thiophene were compared with the ab initio predictions of absorption and VCD spectra obtained with density functional theory using B3LYP/6-31G* basis set for (*S*)-3-(2-methylbutyl)thiophene. This comparison indicates that (+)-3-(2-methylbutyl)-thiophene is of the (*S*) configuration and has six predominant conformations in $CDCl_3$ solution and allows to securely distinguish the vibrational motions of the thiophene ring from those of the substituent moiety.

Introduction

Polythiophenes have attracted much attention because of their significant electrical conductivity and chemical stability.[1] The polymerization of mono or dialkyl thiophenes (with substituents in position 3, or 3 and 4, respectively) yields products[2,3] which can serve as soluble semiconductors.[4] 3-Alkyl-substituted achiral polythiophenes have been studied in detail for their solvatochromic and thermochromic behavior.[5] Optically active polythiophenes, which can be used as stereoselective electrodes and membranes, are noncentrosymmetric and consequently desirable optical and optoelectronic properties are expected for these systems. For these reasons, synthesis and characterization of thiophenes with an optically active alkyl moiety attracted much attention. It has been shown that some sense of chirality onto a conjugated polyheterocycle can be induced by introducing optically active substituents on the backbone.[6] The optically active substituents introduce a perturbation to the chain or to the supramolecular arrangement of several chains and eventually produce an overall chirality of the polymeric systems. (+)-3-(2-Methylbutyl)thiophene (compound **I**) is a member of the rich family of optically active thiophenes, whose polymer was found to be of superior quality probably due to the new synthetic methodology.[7] Chiral poly(3-(2-methylbutyl)thiophene) (polymer **I**) can serve as asymmetric electrodes for chiral electrosynthesis.[8] To understand the relationship between the structure and the properties of the polymer, it is necessary to understand the structure of the repeating unit of the polymer first. (+)-3-(2-Methylbutyl)thiophene **I** was assigned (*S*) configuration by chemical correlation,[8] but its conformations have not been studied before. An independent study of the absolute configuration and predominant conformations of chiral 3-(2-methylbutyl)thiophene by spectroscopic methods would be useful to understand the analogous thiophenes and polythiophenes. The vibrational infrared and Raman spectra[9] are used as structural probes for understanding the structures of polyhexyl and polyoctyl thiophenes. Polythiophenes with chiral substituents have been studied using electronic circular dichroism (ECD), and it has been demonstrated that large ECD signals are observed in mixed solvents (e.g., $CHCl_3/CH_3OH$) or by varying the temperature for solutions in “poor” solvents.[10] The existence of ECD spectra is associated with conformational changes due to different supramolecular arrangements and/or interchain couplings.[10]

Vibrational circular dichroism (VCD) is a powerful and reliable spectroscopic method used to monitor the absolute configuration and predominant conformations of chiral molecules in solution phase. Combined with density functional theory,[11−13] it is possible to use VCD for a confident determination of the absolute configurations and/or conformations in solution phase.[14,15] Indeed the absolute configuration and conformation of some mid-size molecules, polypeptides, and proteins have been successfully determined by the VCD technique. Recently, the absolute configurations and predominant conformations of some chiral molecules such as *tert*-butyl *n*-butyl sulfoxide,[14a] 2,5-dimethyl thiolane and sulfolane,[14b] and *tert*-butylphenylphosphine oxide[14c] have been studied in solution phase using the VCD technique. VCD spectra of some synthetic chiral polymers such as poly-menthyl methacrylate[15a] and poly-3-[5-((±)mentholate)-pentyl]thiophenes[15b] in solution phase have also been reported.

In the present study, we use VCD for the independent verification of the absolute configuration and the determination of the predominant conformations of chiral 3-(2-methylbutyl)-thiophene. One motivation of this stems from the fact that the specific rotation of the starting material (*S*)-1-bromo-2-meth-

---

* Corresponding author. FAX: (615) 322-4936; e-mail: Prasad.L.Polavarapu@vanderbilt.edu

† Vanderbilt University.

‡ Università di Brescia.

§ Istituto di Chimica delle Macromolecole.

10.1021/jp014623q CCC: $22.00

ylbutane is +4.5° at the sodium D line at 21 °C, whereas compound **I** shows a specific rotation of +2.99°. VCD spectra of mono and disubstituted alkylthiophenes, namely (+)-3-(2-methylbutyl)thiophene **I** (compound **I**) and (+)-3,4-di(2-methylbutyl)thiophene **II** (compound **II**) and their corresponding polymers (polymer **I** and polymer **II**) are measured.

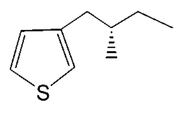

Compound **I**

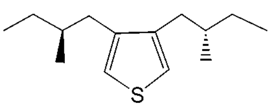

Compound **II**

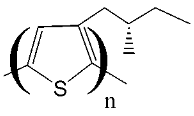

Polymer **I**

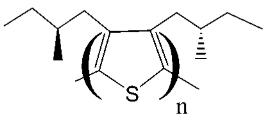

Polymer **II**

State-of-the-art ab initio theoretical VCD investigations of chiral (*R*)-3-(2-methylbutyl)thiophene are undertaken by using the B3LYP/6-31G* basis set. The absolute configurations and predominant conformations of (+)-3-(2-methylbutyl)thiophene **I** are elucidated from these results. The differences in the absorption and VCD spectra of monomers and their polymers are reported.

Experimental Section

Synthesis. Chiral poly[3-(2-methylbutyl)thiophene] was synthesized with Ni(dppp)Cl_2 catalyst using the McCullough method[7] from the corresponding chiral 3-substituted thiophene that had been prepared using enantiomerically pure (*S*)−(+)-1-bromo-2-methylbutane.

Chiral poly[3,4-di(2-methylbutyl)thiophene] was prepared from (+)-3,4-di(2-methylbutyl)thiophene through oxidative polymerization using anhydrous ferric chloride.[10c] The monomer had been prepared from the corresponding 3,4-dibromothiophene and the (*S*)−(+)-1-bromo-2-methylbutane.

Measurements. The average molecular weight ($\overline{M_w}$) determined by GPC in THF against polystyrene standards was 25 000 for polymer **I** and 12 000 for polymer **II** with polydispersity $D = 1.7$ and 1.6, respectively.

The thermogravimetric analysis was made: polymer **I** is stable up to 400 °C and polymer **II** to ca. 350 °C.

The infrared and VCD spectra were recorded on a commercial Fourier transform VCD spectrometer, Chiralir. The VCD spectra were recorded with 3 h data collection time at 4 cm^{-1} resolution. Spectra were measured in $CDCl_3$ solvent at ∼0.25 M and at path length of ∼100 μm for (+)-3-(2-methylbutyl)thiophene and (+)-3,4-di(2-methylbutyl)thiophene. In case of the polymers, a 0.025 g sample was dissolved in 1 mL and 0.5 mL $CDCl_3$, respectively, for polymers **I** and **II**. Using the average molecular weights of the polymers given above, these amounts correspond to 0.164 M and 0.225 M in monomer units, respectively for polymers **I** and **II**. Although these concentrations are comparable to those used for monomers **I** and **II**, the polymers at these concentrations may form aggregates, which is not apparent from the IR and VCD spectra. Measurements at lower concentrations, which require larger path lengths, could not be undertaken due to interference from solvent absorption. The sample was held in a variable path length cell with BaF_2 windows. In the presented absorption spectra, the solvent absorption was subtracted out. In the presented VCD spectra the raw VCD spectrum of the solvent was subtracted.

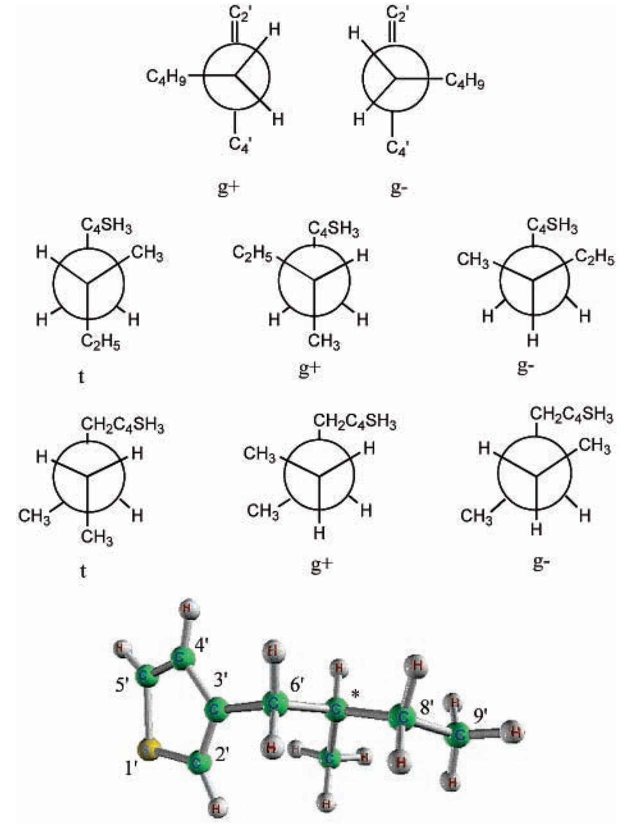

Figure 1. Different conformations of (*R*)-3-(2-methylbutyl)thiophene, based on the dihedral angles of $C_{2'}C_{3'}C_{6'}C^*$, $C_{3'}C_{6'}C^*C_{8'}$, and $C_{6'}C^*C_{8'}C_{9'}$.

Calculations. The ab initio vibrational frequencies, absorption and VCD intensities for (*R*)-3-(2-methylbutyl)thiophene were calculated using the Gaussian 98 program.[13] The calculations used the density functional theory with B3LYP functional[11] and 6-31G* basis set.[16] The procedure for calculating the VCD intensities using DFT theory is due to Cheeseman et al.[12] as implemented in Gaussian 98 program.[13] The theoretical absorption and VCD spectra of (*R*)-3-(2-methylbutyl)thiophene were simulated with Lorentzian band shapes and 8 cm^{-1} full width at half-height. The theoretical VCD spectrum of (*S*)-3-(2-methylbutyl)thiophene was obtained by scaling the intensities of (*R*)-3-(2-methylbutyl)thiophene by −1. Since the ab initio predicted band positions are higher than the experimental values, the ab initio frequencies were scaled with 0.96.

Results and Discussion

The geometries were optimized with the B3LYP/6-31G* basis set using the standard dihedral angles of 0, 60, 120, 180, 240, and 300° for the $C_{2'}C_{3'}C_{6'}C^*$ segment and 60, 180, and 300° for $C_{3'}C_{6'}C^*C_{8'}$ and $C_{6'}C^*C_{8'}C_{9'}$ segments (see Figure 1) of (*R*)-3-(2-methylbutyl)thiophene. These starting geometries converged to 18 conformations, as summarized in Table 1 and shown in Figure 1. Each conformation is labeled with a three-letter designation, with these letters representing the conformation of $C_{2'}C_{3'}C_{6'}C^*$, $C_{3'}C_{6'}C^*C_{8'}$, and $C_{6'}C^*C_{8'}C_{9'}$ dihedral segments, respectively. The converged $C_{2'}C_{3'}C_{6'}C^*$, $C_{3'}C_{6'}C^*C_{8'}$, and $C_{6'}C^*C_{8'}C_{9'}$ dihedral angles, optimized electronic energies, Gibbs energies, and relative populations are listed in Table 1. Thus the g^+tt conformation is expected to be the most stable conformation for isolated 3-(2-methylbutyl)thiophene **I**. From the population composition in Table 1, it is elucidated that at least six conformations have populations greater than 5%. We also notice that the four most probable conformations (g^+tt,

TABLE 1: Conformations and Energies of (*R*)-3-(2-Methylbutyl)thiophene

	starting geom.[b]			converged geom.[b]			energy[c]			
label[a]	$C_{2'}C_{3'}C_{6'}C^*$	$C_{3'}C_{6'}C^*C_{8'}$	$C_{6'}C^*C_{8'}C_{9'}$	$C_{2'}C_{3'}C_{6'}C^*$	$C_{3'}C_{6'}C^*C_{8'}$	$C_{6'}C^*C_{8'}C_{9'}$	electronic	Gibbs	ΔE^d	pop.[e]
a g^+tt	60	180	180	112.1	171.2	−172.7	−749.575160	−749.403875	0	0.244
b g^-g^+t	300	60	180	−113.0	65.0	−171.0	−749.575121	−749.403743	0.083	0.212
c g^+tg^-	60	180	300	111.7	172.1	−66.8	−749.574919	−749.403597	0.174	0.182
d g^-tt	300	180	180	−83.6	172.6	−172.2	−749.574260	−749.403033	0.528	0.100
e g^+g^+t	60	60	180	81.0	63.1	−172.4	−749.574181	−749.402673	0.754	0.068
f g^-tg^-	300	180	300	−84.9	173.3	−66.2	−749.574058	−749.402664	0.760	0.068
g g^+tg^+	60	180	60	110.0	167.2	63.0	−749.573770	−749.401987	1.185	0.033
h $g^-g^+g^+$	300	60	60	−115.0	59.8	63.4	−749.573746	−749.401787	1.310	0.027
i g^+g^-t	60	300	180	96.6	−64.6	−170.4	−749.573406	−749.401531	1.471	0.020
j g^-g^-t	300	300	180	−96.8	−64.2	−168.9	−749.573439	−749.401434	1.532	0.018
k $g^-g^-g^-$	300	300	300	−96.7	−63.8	−63.9	−749.573356	−749.401225	1.663	0.015
l $g^+g^-g^-$	60	300	300	97.3	−63.0	−64.1	−749.573421	−749.401087	1.750	0.013
m g^-tg^+	300	180	60	−86.8	168.6	63.5	−749.572945			
n $g^+g^+g^+$	60	60	60	84.6	61.2	65.8	−749.572798			
o $g^-g^+g^-$	300	60	300	−120.2	70.0	−76.6	−749.572270			
p $g^+g^+g^-$	60	60	300	62.3	71.8	−71.4	−749.571307			
q $g^+g^-g^+$	60	300	60	106.8	−66.2	81.7	−749.569462			
r $g^-g^-g^+$	300	300	60	−84.8	−65.7	82.4	−749.569330			

[a] See Figure 1 for the labels. [b] Dihedral angle. [c] In Hartrees. [d] Relative energy difference, in kcal/mol. [e] Population based on Gibbs energies.

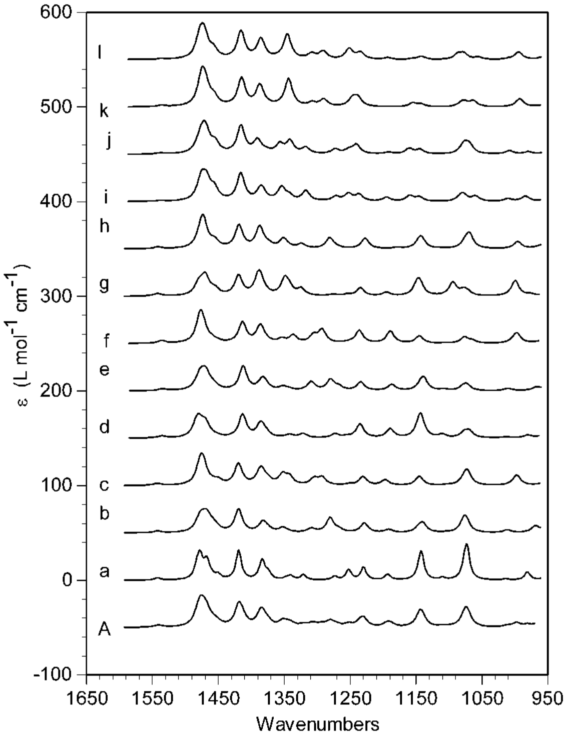

Figure 2. Ab initio vibrational absorption spectra for 12 conformers of 3-(2-methylbutyl)thiophene obtained with the B3LYP/6-31G* basis set. The spectra were simulated with Lorentzian band shapes and 8 cm^{-1} half-widths and frequencies were multiplied with 0.96. The labels on the top 12 traces are the conformation labels (Table 1). The final predicted absorption spectrum, labeled A, is obtained by adding the population weighted absorption spectra of all conformers.

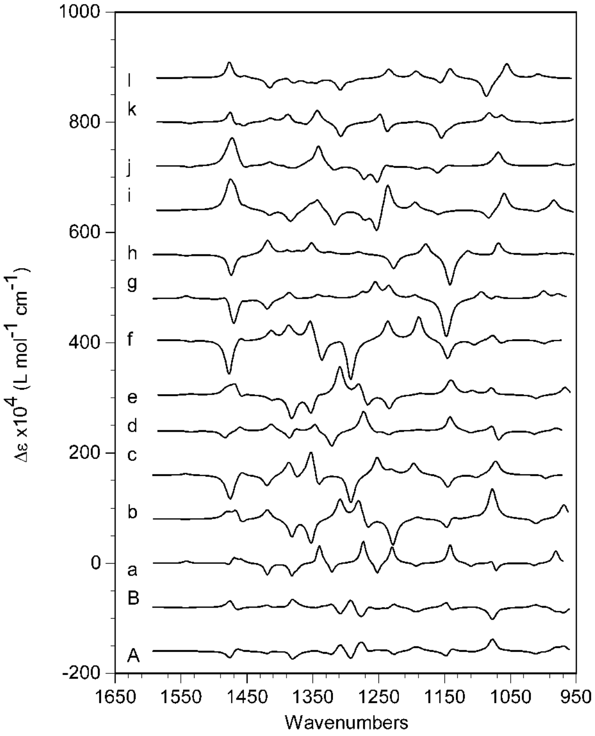

Figure 3. Ab initio VCD spectra for 12 conformers of (*R*)-3-(2-methylbutyl)thiophene obtained with the B3LYP/6-31G* basis set. The spectra were simulated with Lorentzian band shapes and 8 cm^{-1} half-widths and frequencies were multiplied with 0.96. The labels on the top 12 traces are the conformation labels (Table 1). The predicted VCD spectra (A for (*R*) configuration and B for (*S*) configuration) are shown at the bottom; A is obtained by adding the population weighted VCD spectra of all conformers with (*R*) configuration and B is obtained by multiplying the VCD intensities obtained for (*R*) configuration by −1.

g^-g^+t, g^+tg^-, and g^-tt) encompass close to 75% of the possible conformations.

The absorption and VCD intensities were calculated for the 12 most stable conformations at the B3LYP/6-31G* level, and all these conformations were found to have potential energy minima (i.e., all vibrational frequencies are real) at the B3LYP/6-31G* level. The predicted absorption and VCD spectra for all 12 conformations of chiral 3-(2-methylbutyl)thiophene with (*R*) configuration were simulated with 8 cm^{-1} half widths and Lorentzian band shapes (shown in Figures 2 and 3). The unpolarized absorption spectrum is independent of the absolute configuration. The predicted absorption spectrum, obtained as population weighted sum of the absorption spectra of different conformers, is compared to the experimental absorption spectrum in Figure 4. The predicted VCD spectrum for (*S*)-3-(2-methylbutyl)thiophene was obtained by multiplying the VCD intensities obtained for the (*R*) configuration by −1. The population weighted theoretical VCD spectra for chiral 3-(2-methylbutyl)thiophene with (*R*) and (*S*) configurations can be compared to the experimental VCD spectra in Figure 5.

TABLE 2: Comparison of Predicted and Observed Frequencies and Vibrational Assignments for 3-(2-Methylbutyl)thiophene

band no.	exp.[a] (cm^{-1})	pred.[b,c] (cm^{-1})	calc.[b,d] (cm^{-1})	assignment[e]
ν_1	1536	1540	1602	asym. ring deformation, In-plane CH* bend
ν_2	1462	1475	1534	asym. CH_3 deformation, HCH Bend
ν_3	1440*	1453	1511	HCH Bend, Asym. CH_3 deformation
ν_4	1409	1419	1474	sym. ring deformation (C−C and C=C), in-plane CH* bend, CH_2 twist
ν_5	1378	1383	1439	sym. CH_3 deformation
ν_6	1351	1351	1406	CH_2 and CH_3 wag
ν_7	1345	1343	1397	CH_2 and CH_3 wag
ν_8	1323	1321	1375	CH_2 and CH_3 wag
ν_9	1308	1306	1359	CH_2 and CH_3 wag
ν_{10}	1297	1290	1342	CH_2 twist and CH_3 wag
ν_{11}	1285	1280	1331	CH_2 and CH_3 wag
ν_{12}	1258	1251	1303	CH_2 and CH_3 wag
ν_{13}	1241	1231	1280	in-plane CH* bend, CH_2 and CH_3 wag
ν_{14}	1200	1192	1239	CH_2 twist and CH_3 wag, in-plane CH* bend
ν_{15}	1153	1143	1189	CH_2 and CH_3 wag, C−C stretch
ν_{16}	1081	1073	1116	in-plane CH* bend, CH_2 twist
ν_{17}	1031	1012	1053	C−C stretch, CH_2 twist, CH_3 wag
ν_{18}	1015	998	1038	C−C stretch, CH_2 and CH_3 wag

[a] Experimental wavenumbers obtained from the absorption spectrum at concentration of 0.267 M; asterisks (*) denote those may show as shoulders in the spectrum. [b] Band positions from the simulated spectra in Figure 4. [c] Ab initio wavenumbers scaled with 0.96. [d] Unscaled ab initio wavenumbers. [e] Deduced from Gaussview (version 2.1), asterisks (*) denote ring mode.

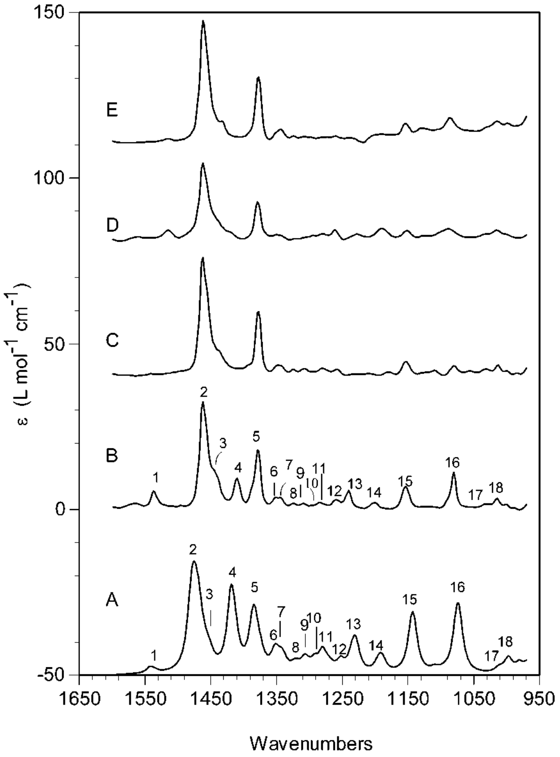

Figure 4. Comparison of the experimental absorption spectra with the predicted (population weighted) absorption (bottom trace) spectra of 3-(2-methylbutyl)thiophene obtained with the B3LYP/6-31G* basis set. The absorption spectra are labeled as (A) predicted spectrum; (B) experimental spectrum for compound **I** (0.25 M in $CDCl_3$, 100 μm path length); (C) experimental spectrum for compound **II** (0.25 M in $CDCl_3$, 100 μm path length); (D) experimental spectrum for polymer **I** (0.025 g/mL in $CDCl_3$, 100 μm path length); and (E) experimental spectrum for polymer **II** (0.050 g/mL in $CDCl_3$, 100 μm path length).

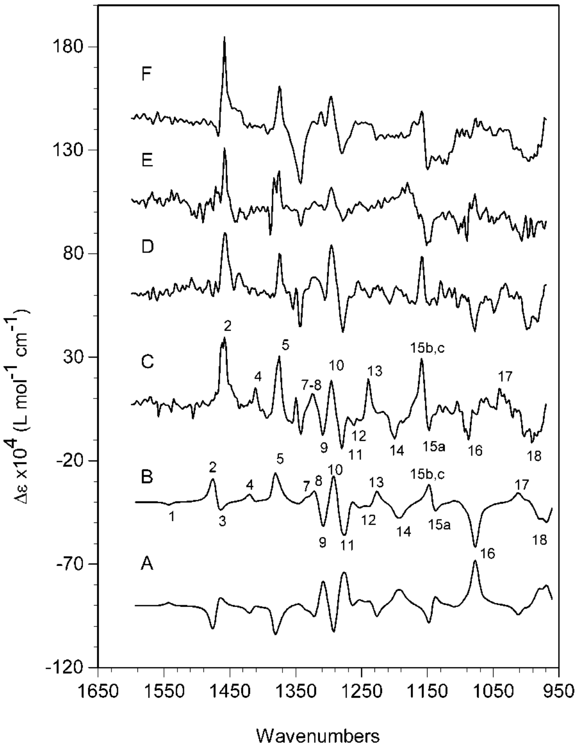

Figure 5. Comparison of the experimental VCD spectra with the predicted (population weighted) VCD (bottom traces) spectra of 3-(2-methylbutyl)thiophene obtained with the B3LYP/6-31G* basis set. The VCD spectra are labeled as (A) predicted spectrum for (*R*) configuration; (B) predicted spectrum for (*S*) configuration (for band #15, the designations a, b, and c are conformation labels (see Table 1)); (C) experimental spectrum for compound **I** (0.25 M in $CDCl_3$, 100 μm path length) where a, b, and c are conformation labels (see Table 1); (D) experimental spectrum for compound **II** (0.25 M in $CDCl_3$, 100 μm path length); (E) experimental spectrum for polymer **I** (0.025 g/mL in $CDCl_3$, 100 μm path length); and (F) experimental spectrum for polymer **II** (0.050 g/mL in $CDCl_3$, 100 μm path length).

The experimental absorption spectra of 3-(2-methylbutyl)thiophene and 3,4-di(2-methylbutyl)thiophene and their polymers obtained in $CDCl_3$ are shown in Figure 4, where the absorption spectrum of the solvent has been subtracted. The absorption bands in the predicted spectrum of 3-(2-methylbutyl)thiophene show one-to-one correspondence with the absorption bands in the experimental spectrum of 3-(2-methylbutyl)thiophene (traces A and B). The notable differences between predicted and experimental absorption spectra are (a) the experimental absorption band (#4) at 1409 cm^{-1} is not as strong as the corresponding band at 1419 cm^{-1} in the predicted spectrum and (b) the experimental band (#10) at 1297 cm^{-1} is not as evident as the corresponding band in predicted spectrum, and the experimental band (#11) at 1285 cm^{-1} is not as strong as the corresponding band in the predicted spectrum. Except for these differences, the experimental spectra in $CDCl_3$ are considered to be in good agreement with the absorption spectrum predicted for 3-(2-methylbutyl)thiophene.

The experimental VCD spectra of (+)-3-(2-methylbutyl)thiophene and (+)-3,4-di(2-methylbutyl)thiophene and their polymers obtained in $CDCl_3$ are shown in Figure 5, where the VCD spectrum of the solvent has been subtracted. The significant VCD bands in the observed (+)-3-(2-methylbutyl)thiophene spectrum (trace C in Figure 5) are 1462 (+, #2), 1409 (+, #4), 1378 (+, #5), 1323 (+, #8), 1308 (−, #9), 1297 (+, #10), 1285 (−, #11), 1241 (+, #13), 1200(−, #14), 1156 (+, #15b,c), 1151 (−, #15a), 1081 (−, #16), 1031 (+, #17), and 1015 (−, #18) cm^{-1}. The major VCD features observed for (+)-3-(2-methylbutyl)thiophene are reproduced in the predicted VCD spectrum of (*S*)-3-(2-methylbutyl)thiophene (trace B in Figure 5). This agreement indicates that (+)-3-(2-methylbutyl)thiophene is of (*S*) configuration.

The experimental absorption and VCD spectra for monomer and polymer of (+)-3-(2-methylbutyl)thiophene are compared in Figures 4 and 5 (traces B and D in Figure 4; traces C and E in Figure 5). The absorption spectrum of polymer **I** is similar to that of compound **I** (see Figure 4), except that (a) the band at 1409 cm^{-1} (#4) in the spectrum of compound **I** shifts left and becomes weakened in the spectrum of polymer **I**; (b) the band at 1536 cm^{-1} (#1) shifts right and becomes broadened; (c) general broadening of other bands is observed in the spectrum for polymer **I**. From the VCD spectrum of polymer **I** (trace E in Figure 5), the positive band at 1409 cm^{-1} (#4) and positive−negative couplet corresponding to bands #13 and 14 [seen in the VCD spectrum of compound **I** (trace C)] disappear, and the negative band #16 becomes weakened. Based on vibrational analysis (Table 2), the two bands (#1, 4) are attributed to ring deformation and bands #13, 14, and 16 have some contribution from in-plane C−H (ring) bending. Ring deformations (#1,4) may be influenced by the delocalization of π electrons in the conjugated polythiophene. C−H bending (ring mode) vibrations are highly influenced by the removal of hydrogen atoms at positions 2 and 5 of thiophene in the formation of the polymer. In addition, the four polymer arrangements, which are indicated with HT-HT (head-to-tail head-to-tail), TT-HT (tail-to-tail head-to-tail), HT-HH (head-to-tail head-to-head), and TT-HH (tail-to-tail head-to-head), may influence the conformational population of the repeating unit. Then the changes in absorption and VCD spectra between monomer and polymer may also come from the interplay between the conformational flexibility of the side chain with the conformational flexibility of the polythiophene backbone. Since there is no significant difference in wavenumbers specified for the side chain of monomer and polymer, and the main VCD patterns of the monomer and polymer are similar (see compound **I** and polymer **I**, and compound **II** and polymer **II**, see Figures 4 and 5), the configurations of the side chain in the two polythiophenes appear the same as those for monomers, and no conformational changes are evident for the repeating units in the formation of polythiophenes. This suggests that the conformations of monomer are mainly determined by the dihedral angles of the alkyl substituent group of thiophene. The aggregation of polymers is also expected to affect conformational stability, but aggregation is not evident in this study.

From the above comparison, significant changes are observed for those bands specific for the backbone (ring deformation and ring C−H bending) in the formation of polymers. The features specific for the side chain, such as CH_3 deformation, HCH bending, CH_2 twist, and CH_3 and CH_2 wag, remain almost the same, except for band broadening and decreasing. These observations suggest that the changes between monomer and polymer partly come from the influence of polymerization on ring deformation and C−H (ring) bending vibrations. However, the influence from other sources, such as conformational flexibility of the side chain and the polythiophene backbone, could not be evaluated herewith.

From the comparison of the experimental absorption and VCD spectra of the two monomers (compounds **I** and **II**, see Figures 4 and 5), bands of compound **II** corresponding to bands #4, 13, and 14 of compound **I** also become weakened. This indicates that the substitution of hydrogen at the 4-position could interrupt the ring mode C−H bending, and the inductive effects of the alkyl chain may influence the ring deformation. The similar VCD sign pattern of compound **I** and compound **II** indicates that (+)-3,4-di(2-methylbutyl)thiophene is also of (*S*) configuration.

Conclusion

The comparison of experimental and ab initio predicted absorption and VCD spectra indicates that (a) (+)-3-(2-methylbutyl)thiophene and (+)-3,4-di(2- methylbutyl)thiophene are of (*S*) configuration, in agreement with the known absolute configuration;[8] (b) the repeating units in polymers **I** and **II** have the same configuration and conformation as those for the corresponding monomers; (c) at least six conformations are present for (*S*)-3-(2-methylbutyl)thiophene in $CDCl_3$ solution, with each contributing more than 5% to conformer population.

Acknowledgment. Grants from the NSF (CHE0092922) and Vanderbilt University are gratefully acknowledged.

Supporting Information Available: Cartesian coordinates for the most stable conformation of (*R*)-3-(2-methylbutyl)thiophene are given.

References and Notes

(1) Patil, A. O.; Heeger, A. J.; Wudl, F. *Chem. Rev.* **1988**, *88*, 183.

(2) Roncali, J.; Garreau, R.; Yassar, A.; Marque, P.; Garnier, F.; Lemaire, M. *J. Phys. Chem.* **1987**, *91*, 6706.

(3) Street, G. B.; Clarke, T. C.; Geiss, R. H.; Lee, V. Y.; Nazzal; A.; Pfluger, P.; Scott, J. C. *J. Phys. Colloq.* **1983**, 599.

(4) Sato, M.; Tanaka, S.; Kaeriyama, K. *J. Chem. Soc., Chem. Commun.* **1986**, 873. Elsenbanmer, R. L.; Jen, K. Y.; Oboodi, R. *Synth. Met.* **1986**, *15*, 169. Hotta, S.; Rughooputh, S. D. D. V.; Heeger, A. J.; Wudl, F. *Macromolecules* **1987**, *20*, 212.

(5) (a) Rughooputh, S. D. D. V.; Hotta, S.; Heeger, A. J.; Wudl, F. *J. Polym. Sci. Polym. Phys.* **1987**, *25*, 1071. (b) Roux, C.; Bergeron, J.-Y.; Leclerc, M. *Macromol. Chem.* **1993**, *194*, 869.

(6) Lemaire, M.; Delabouglise, D.; Garreau, R.; Guy, A.; Roncali, J. *J. Chem. Soc., Chem. Commun.* **1988**, 658. Delabouglise, D.; Garnier, F. *Synth. Met.* **1990**, *39*, 117. Anderson, M.; Ekeblad, P. O.; Hjertberg, T.; Wennerstrom, O.; Inganas, O. *Polymer Commun.* **1991**, *32*, 546. Langeweld-Voss, B. M. W.; Janssen, R. A. J.; Meijer, E. W. *J. Mol. Struct.* **2000**, *521*, 285.

(7) Loewe, R. S.; Khersonsky, S. M.; McCullough, R. D. *Adv. Mater.* **1999**, *11*, 250.

(8) Kotkar, D.; Joshi, V.; Ghosh, P. K. *J Chem. Soc., Chem. Commun.* **1988**, 917.

(9) Zerbi, G.; Chierichetti, B.; Ingänas, O. *J. Chem. Phys.* **1991**, *94*, 4646.

(10) (a) Rughooputh, S. D. D.; Hotta, S.; Heeger, A. J.; Wudl, F. *J. Polym. Sci. Polym. Phys.* **1987**, *25*, 1071. (b) Langeveld-Voss, B. M. W.; Peeters, E.; Janssen, R. A. J.; Meijer, E. W. *Synth. Met.* **1997**, *84*, 611. (c) Lebon, F.; Longhi, G.; Abbate, S.; Catellani, M. *CD spectroscopy of chiral polyalkylthiophenes films and solutions*, XV Italian Conference on Macromolecular Science and Technology, Trieste, Italy, Sept. 2001.

(11) Becke, A. D. *J. Chem. Phys*. **1993**, *98*, 1372. Becke, A. D. *J. Chem. Phys*. **1993**, *98*, 5648.

(12) Cheeseman, J. R.; Frisch, M. J.; Devlin, F. J.; Stephens, P. J. *Chem. Phys. Lett.* **1996**, *252*, 211.

(13) Frisch, M. J.; Trucks, G. W.; Schlegel, H. B.; Scuseria, G. E.; Robb, M. A.; Cheeseman, J. R.; Zakrzewski, V. G.; Montgomery, J. A., Jr.; Stratmann, R. E.; Burant, J. C.; Dapprich, S.; Millam, J. M.; Daniels, A. D.; Kudin, K. N.; Strain, M. C.; Farkas, O.; Tomasi, J.; Barone, V.; Cossi, M.; Cammi, R.; Mennucci, B.; Pomelli, C.; Adamo, C.; Clifford, S.; Ochterski, J.; Petersson, G. A.; Ayala, P. Y.; Cui, Q.; Morokuma, K.; Malick, D. K.; Rabuck, A. D.; Raghavachari, K.; Foresman, J. B.; Cioslowski, J.; Ortiz, J. V.; Stefanov, B. B.; Liu, G.; Liashenko, A.; Piskorz, P.; Komaromi, I.; Gomperts, R.; Martin, R. L.; Fox, D. J.; Keith, T.; Al-Laham, M. A.; Peng, C. Y.; Nanayakkara, A.; Gonzalez, C.; Challacombe, M.; Gill, P. M. W.; Johnson, B.; Chen, W.; Wong, M. W.; Andres, J. L.; Gonzalez, C.; Head-Gordon, M.; Replogle, E. S.; Pople, J. A. *Gaussian 98, Revision A.3*, Gaussian, Inc.: Pittsburgh, PA, 1998.

(14) (a) Drabowicz, J.; Dudziski, B.; Mikoajczyk, M.; Wang, F.; Dehlavi, A.; Goring, J.; Park, M.; Rizzo, C. J.; Polavarapu, P. L.; Biscarini, P.; Wieczorek, M. W.; Majzner, W. R. *J. Org. Chem.* **2001**, *66*, 1122. (b) Wang, F.; Wang, H.; Polavarapu, P. L.; Rizzo, C. J. *J. Org. Chem*. **2001**, *66*, 3507. (c) Wang, F.; Polavarapu, P. L.; Drabowicz, J.; Mikoajczyk, M. *J. Org. Chem.* **2000**, *65*, 7561.

(15) (a) McCann, J.; Tsankov, D.; Hu, N.; Liu, G.; Wieser, H. *J. Mol. Struct.* **1995**, *349*, 309. (b) Lebon, F.; Longhi, G.; Abbate, S.; Catellani, M.; Zhao, C.; Polavarapu, P. L. *Synth. Met.* **2001**, *119*, 75−76.

(16) Hehre, W. J.; Radom, L.; Schleyer, P. v. R.; Pople, J. A. *Ab initio Molecular Orbital Theory;* John Wiley & Sons: New York, 1986.